Supplementary material

Plasma-implanted Ti-doped hematite photoanodes with enhanced photoelectrochemical water oxidation performance

Yong Peng[a,c,d], Qingdong Ruan[b,c], Chun Ho Lam[a], Fanxu Meng[e], Chung-Yu Guan[f], Shella Permatasari Santoso[g], Xingli Zou[h], Edward T. Yu[i], Paul K. Chu[b,c] and Hsien-Yi Hsu[*,a,c,d]

[a] *School of Energy and Environment, City University of Hong Kong, Kowloon Tong, Hong Kong, China*
[b] *Department of Physics, City University of Hong Kong, Tat Chee Avenue, Kowloon, Hong Kong, China*
[c] *Department of Materials Science and Engineering, City University of Hong Kong, Tat Chee Avenue, Kowloon, Hong Kong, China*
[d] *Shenzhen Research Institute of City University of Hong Kong, Shenzhen, 518057, China*
[i] *Microelectronics Research Center, Department of Electrical and Computer Engineering, the University of Texas at Austin, Austin, Texas 78758*

***Corresponding author:**

Hsien-Yi Hsu, E-mail: sam.hyhsu@cityu.edu.hk

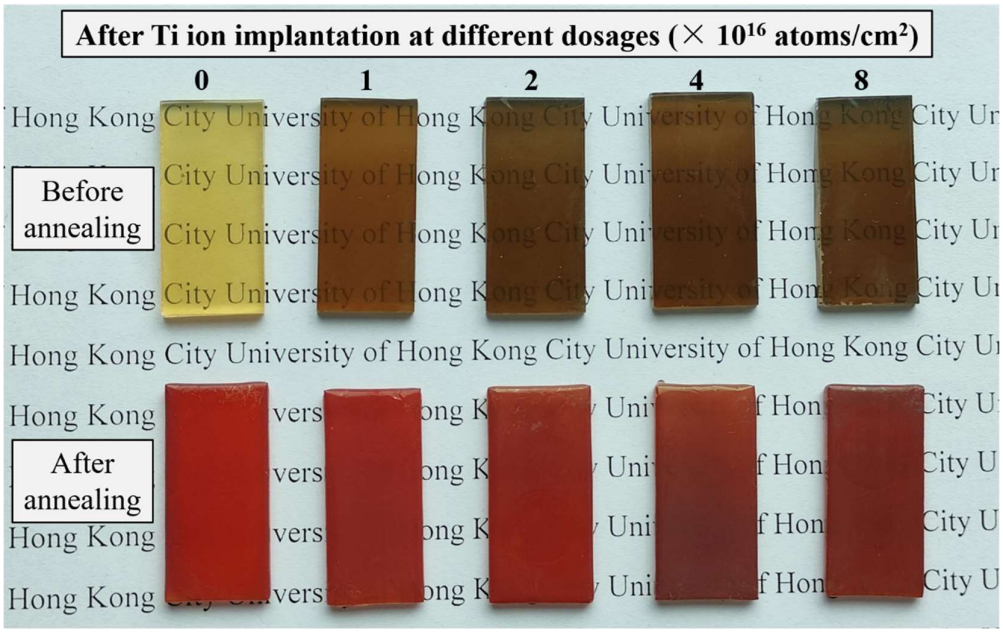

Figure S1. Photographs of β-FeOOH (before annealing) and α-Fe_2O_3 (after annealing) after the implantation with different dose of titanium ions.

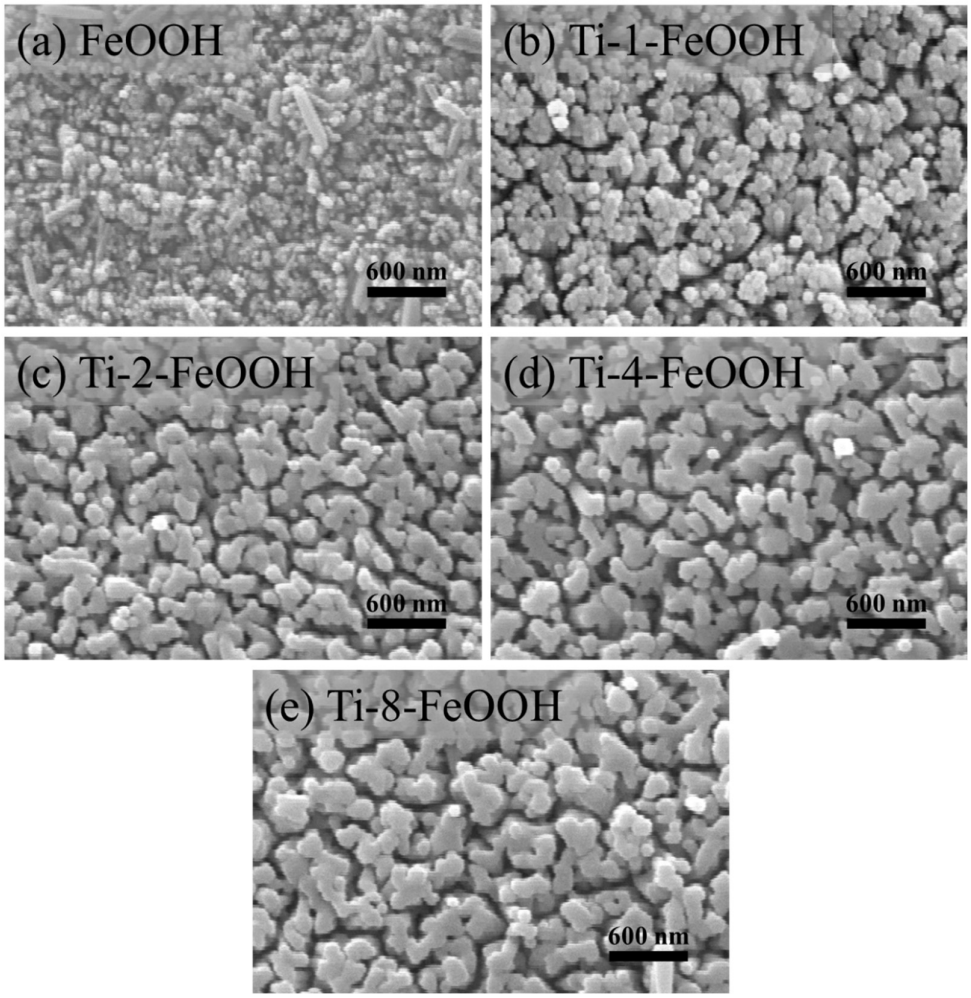

Figure S2. SEM images of titanium ion implanted β-FeOOH at different implantation doses: (a) FeOOH, (b) Ti-1-FeOOH, (c) Ti-2-FeOOH, (d) Ti-4-FeOOH and (e) Ti-8-FeOOH.

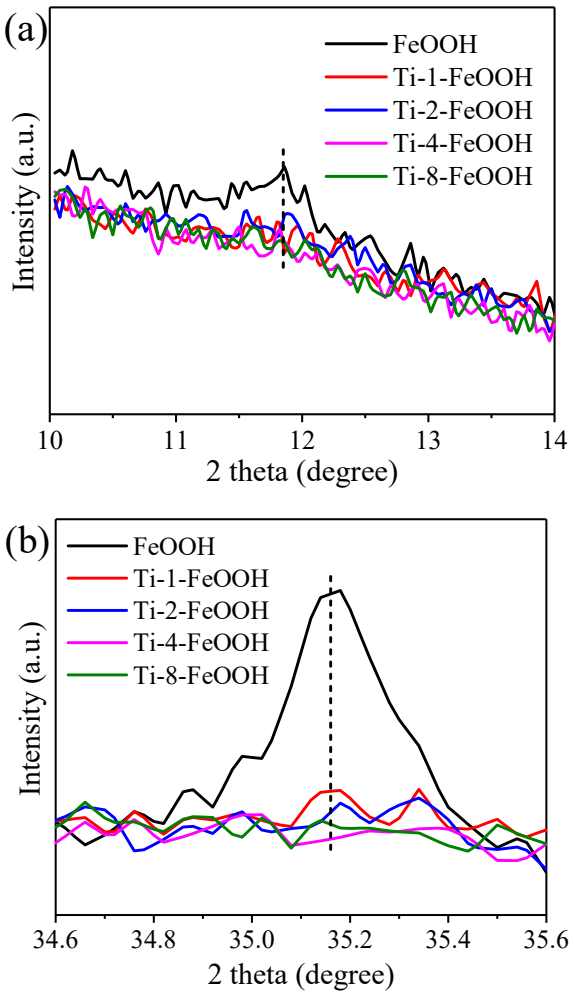

Figure S3. Magnified XRD patterns of titanium ion implanted β-FeOOH at the range of (a) 10 to 14 degree, and (b) 34.6 to 35.6 degree.

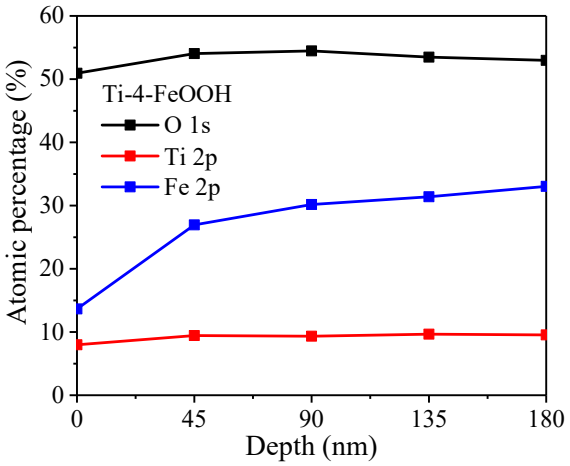

Figure S4. Depth profile of Ti-4-FeOOH before post-annealing process.

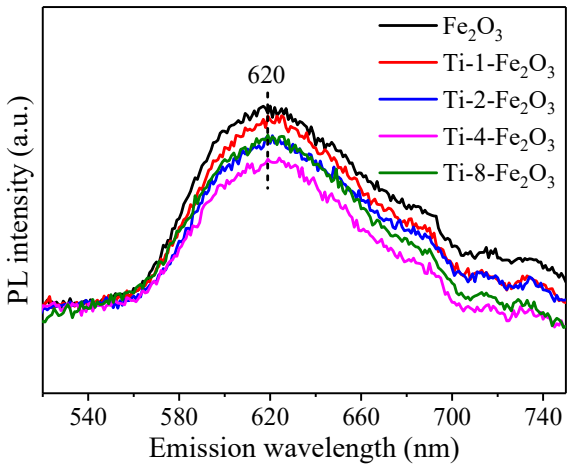

Figure S5. Photoluminescence spectra of titanium ion implanted α-Fe_2O_3 at different doses.

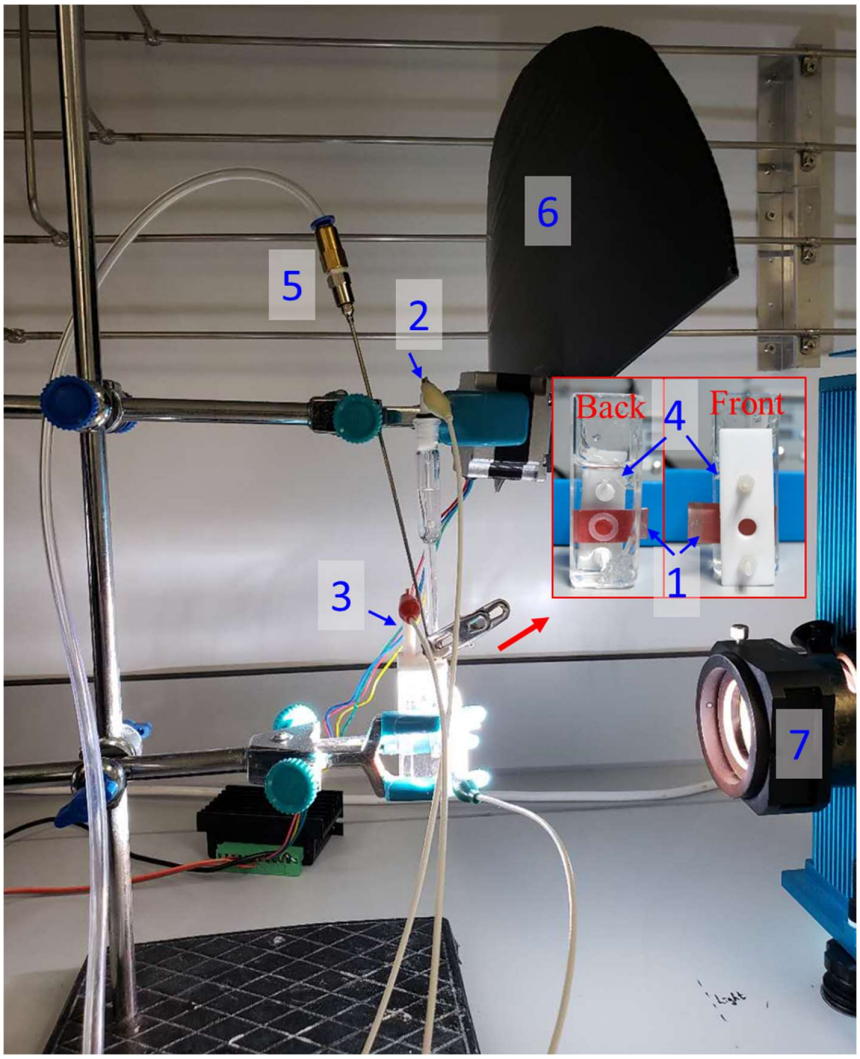

Figure S6. Self-designed three-electrode system for electrochemical measurements: (1) the hematite photoanode as a working electrode, (2) Ag/AgCl (3 M KCl) with a salt bridge (3 M KCl) as a reference electrode, (3) Pt wire as a counter electrode, (4) 1 M NaOH (pH 13.6) served as an electrolyte, (5) nitrogen purging for the removal of oxygen during the measurements, (6) light barrier for the collection of chopped curves if needed, and (7) 300-W xenon lamp as a light source.

Table S1. The Raman intensity ratio of the peak at 660 cm^{-1} to the peak at 610 cm^{-1} for pristine α-Fe_2O_3 and titanium ion implanted α-Fe_2O_3.

Samples	Peak height at 610 cm^{-1}	Peak height at 660 cm^{-1}	Ratio (I_{660}/I_{610})
Fe_2O_3	3.141	0.821	0.26
Ti-1-Fe_2O_3	2.695	1.616	0.60
Ti-2-Fe_2O_3	3.307	2.096	0.63
Ti-4-Fe_2O_3	3.526	3.057	0.87
Ti-8-Fe_2O_3	1.547	1.260	0.81

Table S2. EIS fitting parameters for pristine α-Fe_2O_3 and titanium ion implanted α-Fe_2O_3.

Samples	R_s (Ω)	R_{ct} (Ω)	CPE-T (F)	CPE-P
Fe_2O_3	492	1441	3.01E-05	0.708
Ti-1-Fe_2O_3	503	1087	9.74E-06	0.855
Ti-2-Fe_2O_3	589	1048	1.69E-05	0.794
Ti-4-Fe_2O_3	686	999	2.20E-05	0.770
Ti-8-Fe_2O_3	455	1119	1.35E-05	0.862

Table S3. Calculated charge carrier densities of as-prepared and titanium ion implanted α-Fe_2O_3 based on Mott-Schottky plots.

Samples	Donor density ($\times 10^{25}$ m^{-3})
Fe_2O_3	9.6
Ti-1-Fe_2O_3	10.8
Ti-2-Fe_2O_3	18.4
Ti-4-Fe_2O_3	71.0
Ti-8-Fe_2O_3	10.1

Table S4. Current densities of pristine Fe_2O_3 and titanium ion implanted Fe_2O_3 films at 1.23 V and 1.5 V versus RHE under 1-sun illumination.

Samples	Current density (mA cm^{-2})	
	@1.23 V vs. RHE	@1.5 V vs. RHE
Fe_2O_3	0.34	0.67
Ti-1-Fe_2O_3	0.40	0.84
Ti-2-Fe_2O_3	0.53	1.01
Ti-4-Fe_2O_3	0.55	1.07
Ti-8-Fe_2O_3	0.36	0.77